

Journal of Materials Chemistry C

Accepted Manuscript



This article can be cited before page numbers have been issued, to do this please use: F. Tong, Z. Chen, X. Lu and Q. Lu, *J. Mater. Chem. C*, 2017, DOI: 10.1039/C7TC02958F.



This is an Accepted Manuscript, which has been through the Royal Society of Chemistry peer review process and has been accepted for publication.

Accepted Manuscripts are published online shortly after acceptance, before technical editing, formatting and proof reading. Using this free service, authors can make their results available to the community, in citable form, before we publish the edited article. We will replace this Accepted Manuscript with the edited and formatted Advance Article as soon as it is available.

You can find more information about Accepted Manuscripts in the [author guidelines](#).

Please note that technical editing may introduce minor changes to the text and/or graphics, which may alter content. The journal's standard [Terms & Conditions](#) and the ethical guidelines, outlined in our [author and reviewer resource centre](#), still apply. In no event shall the Royal Society of Chemistry be held responsible for any errors or omissions in this Accepted Manuscript or any consequences arising from the use of any information it contains.



Journal of Materials Chemistry C

PAPER

Thermostable birefringent copolyimide films based on azobenzene-containing pyrimidine diamines†

Faqin Tong, Zhao Chen, Xuemin Lu*, and Qinghua Lu*

Received 00th January 20xx,
Accepted 00th January 20xx

DOI: 10.1039/x0xx00000x

www.rsc.org/

Azobenzene (azo)-containing polymers have attracted continuous attention due to their excellent photosensitivity. However, practical applications of their photo-induced birefringence have been hampered by low thermal stability. In this work, we report a series of polyimides synthesized by a low-temperature co-polycondensation of azo-containing pyrimidyl diamine, 4,4'-diaminodiphenyl ether, and 4,4'-oxydiphthalic anhydride. The obtained co-polyimides (co-PIs) show good thermal stability, with high glass transition temperatures (T_g) of more than 200 °C and 5% weight loss temperatures ($T_{5\%}$) as high as about 400 °C in nitrogen. Their photo-induced birefringence (Δn) has been determined as 0.013 at room temperature and up to 0.017 at 100 °C. The photo-induced reorientation property of the as-prepared highly thermostable azo-PIs is expected to have wide applications in image recording and electro-optical devices.

1. Introduction

The azobenzene (azo) unit is extremely well-known and widely investigated because of its unique photoresponse feature. Under light irradiation, *trans*-to-*cis* isomerization of the azo group leads to changes in geometrical structure, dipole moment, and spatial volume at the molecular level, and furthermore in refractive index and colors at the macroscopic level.¹ Azo-containing polymers have been extensively studied due to their excellent photosensitivity and corresponding diverse promising applications in fields such as high-density optical data storage, liquid-crystal devices, optical waveguides, diffractive elements, and so forth.^{2–6} However, for most azo-containing polymers, low stability of their photo-induced anisotropy under high-temperature conditions is their main drawback, which results from the poor thermal stability of most polymer matrices, such as polyacrylate,^{7, 8} poly(methyl methacrylate) (PMMA),^{9, 10} and polyethylene terephthalate (PET),¹¹ which generally have low T_g values of 80–150 °C.

Polyimides (PIs), especially aromatic PIs, which have excellent thermal, mechanical, and electrical properties, as well as good chemical resistance and low susceptibility to laser damage, represent good polymer matrix candidates for photoresponsive materials with high thermal stability. Azo-containing PIs (azo-PIs) have been reported as photosensitive materials, for example, as photoalignment layers for liquid crystals,¹² photomechanical response materials,¹³ and photo-induced surface relief gratings.¹⁴ Zlatanova et al.¹⁵ reported

that a PI system doped with methyl orange dye displayed photosensitivity, although the photo-induced birefringence, Δn , was only ca. 0.00038 owing to the steric hindrance of the PI. Schab-Balcerzak et al.^{16, 17, 18} reported a series of poly(ester imide)s and poly(ether imide)s with azo units as side chains, which showed high birefringence up to 0.02. However, incorporation of long alkoxy spacers reduced the T_g values to 140–170 °C. Konieczkowska et al.^{19, 20} reported poly(amideimide)s with two azochromophores per structural unit, which showed a high birefringence up to 0.075 and a high T_g values of 280 °C. However, the thermal stability of the photo-induced birefringence of the polymers was not investigated. Thus, from a practical point of view, there is still great demand for the design and construction of azo-PIs with higher thermal stability and photo-induced birefringence.

As reported, the introduction of heterocyclic aromatic structures into the main chains of PIs is considered to be an effective approach for improving thermal resistance. Various novel PI materials with heterocyclic structures in their main chains, such as pyridine,²¹ triazine,²² naphthalene,²³ furan,²⁴ or pyrimidine,²⁵ have been reported. For example, Chen *et al.* systematically studied single electro-spun nanofibers and aligned nanofiber belts from co-PIs with pyrimidine units,²⁶ and confirmed that incorporation of rigid pyrimidine units improved the thermal performance of PI. Meanwhile, pyrimidine rings and sulfur atoms with high molar refractions have been incorporated to improve the optical properties of PIs.^{27, 28, 29} High optical transparency is the principal concern in designing optical polymers for high-performance components for advanced display devices.

Polymers containing azo moieties in their side chains generally require a spacer between the rigid polymer main chain and the azo groups to impart the necessary flexibility for the required movement.³⁰ Stumpe and co-workers studied the

School of Chemistry and Chemical Engineering, Shanghai Key Laboratory of Electrical Insulation and Thermal Aging, Shanghai Jiao Tong University, Shanghai 200240, P. R. China. *E-mail address: qhlu@sjtu.edu.cn, xueminlu@sjtu.edu.cn; Tel and Fax +86-021-54747535

† Electronic Supplementary Information (ESI) available: See DOI: 10.1039/x0xx00000x

effect of spacer length of the azo unit on the reorientation behavior of liquid-crystalline polymers.³¹ The orientational order increased or decreased, depending on the enthalpic stability of the mesophase, which changed with spacer length. However, to the best of our knowledge, photo-induced birefringence in azo-PIs containing azo side chains with different spacer lengths has not hitherto been studied.

At present, there is scarce report on the photo-induced birefringence in the polyimides containing pyrimidine aromatic structures. In this work, we have designed and synthesized a series of novel photosensitive azo-PIs by polycondensation of azo-containing pyrimidyl diamine, 4,4'-diaminodiphenyl ether (ODA), and 4,4'-oxydiphthalic anhydride (ODPA). Different alkyl spacer lengths between the main chain and the azo unit were introduced in the side chains with thioether linkages to optimize the photo-induced birefringence. The level and dynamics of the generated birefringence, as well as its thermal stability, were further investigated.

2. Experimental

2.1. Materials

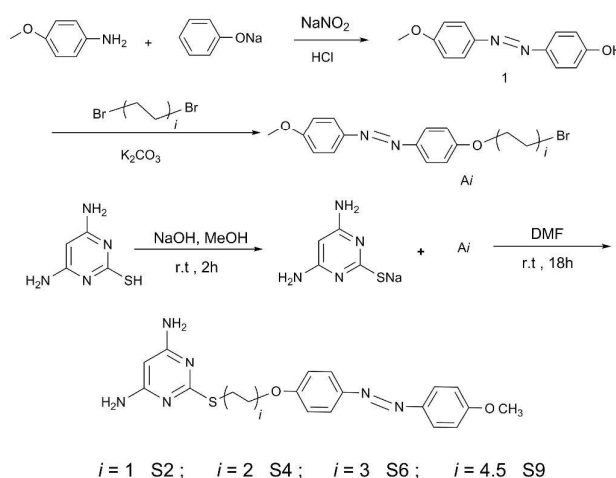
Sodium nitrite, phenol, potassium carbonate, 4-methoxyaniline, sodium hydroxide, and hydrochloric acid were purchased from Sinopharm Chemical Reagent Co. (Shanghai, China). 4,6-Diamino-2-mercapto-pyrimidine was purchased from Aladdin (Shanghai, China). 1,2-Dibromoethane, 1,4-dibromobutane, 1,6-dibromohexane, and 1,9-dibromononane were obtained from J&K Reagent Co. (Beijing, China). 4,4'-Diaminodiphenyl ether (ODA) was purchased from Alfa Aesar (Ward Hill, MA, USA) and purified by recrystallization from ethanol. 4,4'-Oxydiphthalic anhydride (ODPA; >99%, Suzhou Yacoo Chemical Reagent Corporation, Jiangsu, China) was purified by recrystallization from acetic anhydride and dried under vacuum prior to use. *N,N'*-Dimethylformamide (DMF) and *N,N'*-dimethylacetamide (DMAc) were distilled under reduced pressure after stirring over calcium hydride for 24 h and stored over 4 Å molecular sieves before use.

2.2. Characterization

Proton and carbon nuclear magnetic resonance (¹H NMR and ¹³C NMR) spectra were recorded on a Varian Mercury Plus 400 MHz spectrometer (Varian, Palo Alto, CA, USA) using deuterated dimethylsulfoxide ([D₆]DMSO) or chloroform (CDCl₃) as solvent at room temperature, and the chemical shifts were referenced relative to tetramethylsilane (TMS). Attenuated total reflection–Fourier-transform infrared (ATR-FTIR) spectra were recorded on a Perkin-Elmer Spectrum 100 FTIR spectrophotometer (Perkin Elmer, Norwalk, CT, USA). High-resolution mass spectrometric (HRMS) analysis was performed on a Solarix-70FT-MS Fourier-transform ion cyclotron resonance mass spectrometer (MS) (Bruker Daltonics, Karlsruhe, Germany). Elemental analyses were performed using Vario EL Cube. Molecular weights and polydispersities were estimated using a Perkin-Elmer Series 200 gel permeation chromatograph (GPC) at 40 °C equipped with two linear mixed-B columns (Polymer Lab Corporation;

pore size: 10 μm, column size: 300 × 7.5 mm) and a refractive index detector. DMF (0.03 mol L⁻¹ LiBr and 0.03 mol L⁻¹ H₃PO₄) and polystyrene were used as the eluent (elution rate: 1.0 mL min⁻¹) and the calibration standard, respectively. Thermogravimetric analysis (TGA) was performed using a TA TGA Q5000IR instrument (TA Instruments, Inc., New Castle, DE, USA). Samples were heated at a rate of 20 °C min⁻¹ from room temperature to 700 °C in nitrogen. Differential scanning calorimetry (DSC) was performed on a TA DSC Q2000 instrument at a heating rate of 10 °C min⁻¹ in nitrogen. Absorption spectra of PI films were measured on a Perkin-Elmer Lambda 750 UV/Vis spectrophotometer. Tensile tests were performed on samples of dimensions 30 mm×3 mm×20 μm at 25 °C using an Instron 4465 test machine (Instron Corp., Canton, MA, USA).

2.3. Monomer Synthesis



Scheme 1. Synthetic route to the diamine monomers.

4-Hydroxy-4'-methoxyazobenzene (1) was synthesized according to the reported method.³²

1-Bromo-2-(4-methoxyazobenzene-4'-oxy)ethane (A1)³³: A mixture of **1** (4.56 g, 0.02 mol), 1,2-dibromoethane (7.44 g, 0.04 mol), potassium carbonate (4.2 g, 0.03 mol), and acetone was stirred under reflux for 24 h. The reaction mixture was filtered when hot, and the residue was washed with acetone. The acetone was removed under reduced pressure and petroleum ether was added to the concentrated organic extract. The resulting precipitate was collected and dried. The crude product was recrystallized from ethanol. Yield: 5.2 g, 78%. ¹H NMR (400 MHz, CDCl₃, δ (ppm)): 7.93 (ArH, 4H), 7.01 (ArH, 4H), 4.38 (OCH₂, 2H), 3.90 (CH₃O, 3H), 3.70 (CH₂Br, 2H).

1-Bromo-4-(4-methoxyazobenzene-4'-oxy)butane (A2): **A2** was prepared by a procedure analogous to that described for **A1**. The product was obtained by recrystallization from ethanol in 72% yield. ¹H NMR (400 MHz, CDCl₃, δ (ppm)): 7.90 (ArH, 4H), 7.01 (ArH, 4H), 4.10 (OCH₂, 2H), 3.91 (CH₃O, 3H), 3.52 (CH₂Br, 2H), 2.10–1.98 (C₂H₄CH₂Br, 4H).

1-Bromo-6-(4-methoxyazobenzene-4'-oxy)hexane (A3): **A3** was prepared by a procedure analogous to that described for **A1**. After recrystallization from ethanol, the final **A3** was obtained as a yellow solid in 80% yield. ¹H NMR (400 MHz,

CDCl_3 , δ (ppm): 7.95 (ArH, 4H), 7.02 (ArH, 4H), 4.07 (OCH_2 , 2H), 2H), 3.91 (CH_3O , 3H), 3.46 (CH_2Br , 2H), 1.94 ($\text{CH}_2\text{CH}_2\text{Br}$, 2H), 1.86 (OCH_2CH_2 , 2H), 1.66–1.46 ($\text{OCH}_2\text{CH}_2\text{C}_2\text{H}_4\text{CH}_2\text{CH}_2\text{Br}$, 4H).

1-Bromo-9-(4-methoxyazobenzene-4'-oxy)nonane (A4.5): **A4.5** was prepared by a procedure analogous to that described for **A1**. The product was obtained by recrystallization from ethanol in 68% yield. ^1H NMR (400 MHz, CDCl_3 , δ (ppm)): 7.91 (ArH, 4H), 7.02 (ArH, 4H), 4.07 (OCH_2 , 2H), 3.91 (CH_3O , 3H), 3.44 (CH_2Br , 2H), 1.95–1.34 ($\text{C}_7\text{H}_{14}\text{CH}_2\text{Br}$, 14H).

2-((2-(4-Methoxyazobenzene-4'-oxy)ethyl)thio)pyrimidine-4,6-diamine (S2)³⁴: In a flask, 4,6-diamino-2-mercaptopyrimidine (1.42 g, 10 mmol), aqueous NaOH (0.25 M, 42 mL), and methanol (40 mL) were combined. The reaction mixture was stirred with a magnetic stirrer at room temperature for 2 h to form the corresponding sodium thiolate salt. The solvent was then evaporated under vacuum. The dry sodium thiolate salt was dissolved in dry DMF (60 mL), and **A1** (3.67 g, 11 mmol, 1.1 equiv) was added. The resulting yellow solution was stirred at room temperature for 12 h. The progress of the reaction was monitored by thin-layer chromatography (TLC) ($\text{CH}_2\text{Cl}_2/\text{MeOH}$, 19:1). After completion, the reaction was quenched with water, and the mixture was extracted with CH_2Cl_2 . The organic layer was collected and concentrated. The crude material was purified by flash chromatography ($\text{CH}_2\text{Cl}_2/\text{MeOH}$, 9:1) to give the desired product. The product was obtained as a yellow solid in 78.3% yield (3.1 g), m.p. 215–216 °C. ^1H NMR (400 MHz, $[\text{D}_6]$ DMSO, δ (ppm)): 7.85 (ArH, 4H), 7.13 (ArH, 4H), 6.13 (NH_2 , 4H), 5.13 (ArH, 1H), 4.29 (OCH_2 , 2H), 3.86 (OCH_3 , 3H), 3.39 (SCH_2 , 2H). High-resolution MS (ESI, m/z): $[M^+]$ calcd for $\text{C}_{19}\text{H}_{20}\text{N}_6\text{O}_2\text{S}$: 396.14; found: 396.14.

2-((4-(4-Methoxyazobenzene-4'-oxy)butyl)thio)pyrimidine-4,6-diamine (S4): Diamine **S4** was prepared according to an experimental procedure analogous to that described for **S2**, except that the reaction time was 16 h in DMF. After recrystallization from ethanol, the final **S4** was obtained as a yellow solid in 80% yield, m.p. 196–197 °C. ^1H NMR (400 MHz, $[\text{D}_6]$ DMSO, δ (ppm)): 7.84 (ArH, 4H), 7.11 (ArH, 4H), 6.06 (NH_2 , 4H), 5.15 (ArH, 1H), 4.09 (OCH_2 , 2H), 3.86 (OCH_3 , 3H), 3.04 (SCH_2 , 2H), 1.86 ($\text{CH}_2\text{CH}_2\text{O}$, 2H), 1.77 (SCH_2CH_2 , 2H). High-resolution MS (ESI, m/z): $[M^+]$ calcd for $\text{C}_{21}\text{H}_{24}\text{N}_6\text{O}_2\text{S}$: 424.17; found: 424.17.

2-((6-(4-Methoxyazobenzene-4'-oxy)hexyl)thio)pyrimidine-4,6-diamine (S6): Diamine **S6** was prepared according to an experimental procedure analogous to that described for **S2**. After recrystallization from ethanol, the final **S6** was obtained as a yellow solid in 85% yield, m.p. 192–193 °C. ^1H NMR (400 MHz, $[\text{D}_6]$ DMSO, δ (ppm)): 7.84 (ArH, 4H), 7.11 (ArH, 4H), 6.07 (NH_2 , 4H), 5.13 (ArH, 1H), 4.07 (OCH_2 , 2H), 3.86 (OCH_3 , 3H), 2.98 (SCH_2 , 2H), 1.77 (OCH_2CH_2 , 2H), 1.62 (SCH_2CH_2 , 2H), 1.41–1.44 ($\text{OCH}_2\text{CH}_2\text{C}_2\text{H}_4\text{CH}_2\text{CH}_2\text{S}$, 4H). High-resolution MS (ESI, m/z): $[M^+]$ calcd for $\text{C}_{23}\text{H}_{28}\text{N}_6\text{O}_2\text{S}$: 452.57; found: 452.19.

2-((9-(4-Methoxyazobenzene-4'-oxy)nonyl)thio)pyrimidine-4,6-diamine (S9): Diamine **S9** was prepared according to an experimental procedure analogous to that described for **S2**. After recrystallization from ethanol, the final **S9** was obtained as a yellow solid in 80% yield, m.p. 181–183 °C. ^1H NMR (400 MHz, $[\text{D}_6]$ DMSO, δ (ppm)): 7.84 (ArH, 4H), 7.10 (ArH, 4H),

6.06 (NH_2 , 4H), 5.14 (ArH, 1H), 4.07 (OCH_2 , 2H), 3.86 (OCH_3 , 3H), 2.94 (SCH_2 , 2H), 1.73–1.35 ($\text{OCH}_2\text{C}_7\text{H}_{14}\text{CH}_2\text{S}$, 14H). High-resolution MS (ESI, m/z): $[M^+]$ calcd for $\text{C}_{26}\text{H}_{34}\text{N}_6\text{O}_2\text{S}$: 494.25; found: 494.25.

The chemical structures of the diamines were confirmed by melting point analysis (data in the Experimental part) and by ^1H and ^{13}C NMR. All of the spectroscopic data obtained were consistent with the proposed structures. The ^1H NMR peaks of the respective diamines could be unequivocally assigned, as shown in Figure 1. Their ^{13}C NMR spectra are provided in

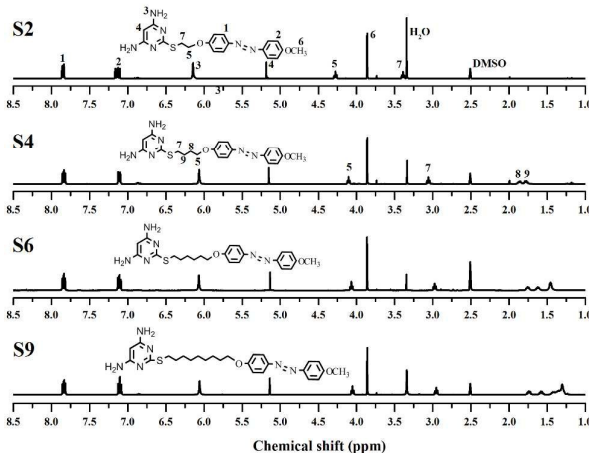
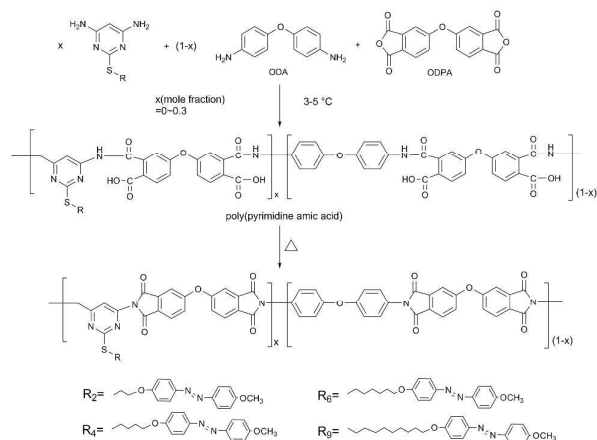


Figure 1. ^1H NMR spectra of the diamines in $[\text{D}_6]$ DMSO.

Figure S1.

2.4. Preparation of azo-PIs

In this work, **Sn**/ODA/ODPA with a molar ratio of 0–0.3:1–0.7:1 was applied to prepare **PIx-Sn** (Scheme 2). Here, “**x**” in **PIx-Sn** denotes the molar ratio of the azo-containing pyrimidyl diamine to the ODA in the co-polymer, and “**n**” denotes the spacer length of the alkyl chain. The synthesis of azo-PI is exemplified by the case of **PI1-S6**. **S6** (0.4526 g, 1 mmol) and ODA (1.8022 g, 9 mmol) were dissolved in DMAc (16.12 g) in a 100 mL three-necked flask fitted with a mechanical stirrer and a nitrogen inlet. After complete dissolution of the diamine, the flask was cooled to 5 °C in an ice bath. A solution of ODPA (3.1022 g, 10 mmol) in DMAc (5.31 g) was added, and the resultant mixture was stirred under a gentle flow of dry nitrogen. After 10 h, a viscous, homogeneous solution of



Scheme 2. Synthetic route to all of the azo-PIs.

polyamic acid (PAA) had formed.

PAA₁-S6: ¹H NMR (400 MHz, [D₆] DMSO, δ(ppm)): 1.41–1.44 (OCH₂CH₂C₂H₄CH₂CH₂S, 4H), 1.62 (SCH₂CH₂, 2H), 1.77 (OCH₂CH₂, 2H), 2.98 (SCH₂, 2H), 3.86 (OCH₃, 3H), 4.07 (OCH₂, 2H), 5.13 (ArH, 1H), 7.11 (ArH, 4H), 7.24 (ArH, 4H), 7.53 (ArH, 4H), 7.67 (ArH, 4H), 7.81 (ArH, 4H), 7.95 (ArH, 4H), 10.37 (CONH, 2H), 10.43 (CONH, 2H), 13.03 (COOH, 4H). (**PI₁-S6**: Anal. Calcd. for C₂₉₁H₁₅₆N₂₄O₆₁S (4993): C, 69.93%; N, 6.73%; H, 3.12%. Found: C, 68.52%; N, 7.46%; H, 3.52%.)

The ¹H NMR of other PAAs and the elemental analysis of the corresponding azo-PIs are shown in supporting information.

2.5. Preparation of azo-PI films

Synthesis of the azo-PI films is exemplified by the case of **PI₁-S6**. **PI₁-S6** film was obtained by thermal imidization of a PAA solution cast onto a glass plate. This involved a preheating program (70 °C/1 h, 90 °C/2 h, 110 °C/1 h) followed by the imidization procedure (200 °C/2 h, 220 °C/2 h, 250 °C/2 h) to produce a fully imidized PI film. The **PI₁-S6** film was exfoliated by placing the glass plate in hot water. The other azo-PI films were prepared analogously.

2.6. Photo-induced birefringence

The experimental set-up for measurements of photo-induced birefringence is shown schematically in Figure 2. He-Ne laser beam (λ = 632.8 nm) was used as a probe light beam. Any light-imposed molecular reorientation in an azo-functionalized polymer film results in the creation of in-plane optical anisotropy, that is, birefringence. A continuous linearly polarized 405 nm laser was used as the pump light, and the beam intensity was about 200 mW/cm². The thickness for the polymer films utilized in the photoinduced birefringence measurement was 20 μm by means of a film thickness measuring instruments. The absorption coefficient value of PI films at the wavelength of 405 nm was 1.73 × 10³ cm⁻¹, 2.62 × 10³ cm⁻¹, and 2.73 × 10³ cm⁻¹ for **PI₁-S6**, **PI₂-S6**, and **PI₃-S6**, respectively. The values increased with the amount of pyrimidyl diamine increasing, which can be attributed to the absorption of azo chromophore. The birefringence (Δ*n*) was calculated according to the following equation:

$$I = I_0 \sin^2(\pi \Delta n d / \lambda)$$

where *I* is transmitted intensity of the probing light through crossed-polarizer set-up, *I*₀ is the intensity of the probe beam, λ is the wavelength of the probe light, and *d* is the thickness of the film.

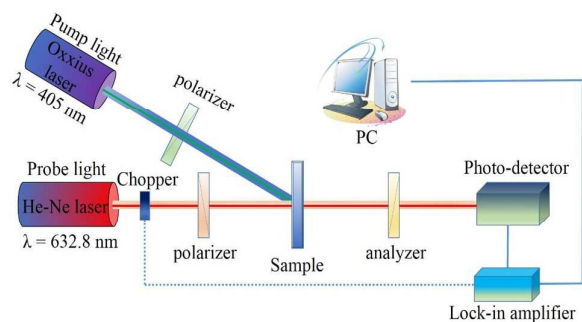


Figure 2. Experimental set-up for measuring photo-induced birefringence.

3. Results and discussion

3.1. Synthesis of azo-PIs

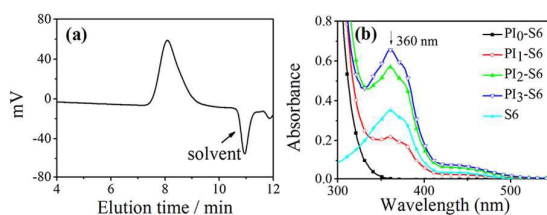


Figure 3. (a) GPC chromatogram of **PAA₃-S6**; eluent: DMF containing LiBr and H₃PO₄. (b) UV-vis absorption spectra of the PAAs of **PI_x-S6** in DMAC solution (concentration 0.05 mg/mL) and **S6** in DMAc solution (concentration 0.008 mg/mL).

The pyrimidine-containing azo-PIs were synthesized by reaction of **S_x**/ODA/ODPA systems in molar proportions of 0–0.3:1–0.7:1 according to a conventional two-step procedure as shown in Scheme 2. The molecular weights of the PAAs were measured by GPC and are summarized in Table S1. The GPC trace for **PAA₃-S6** is shown in Figure 3(a). No peaks due to small molecules were observed in the GPC trace for **PAA₃-S6**, indicating that the pyrimidyl diamine had been covalently incorporated into the polymer chains. UV absorbance spectra of the corresponding PAAs of the respective azo-PIs are shown in Figure 3(b), and those of the others are shown in Figures S2–S4. The UV absorption intensity at 360 nm, corresponding to π–π* electronic transition of the azo chromophore, increased in the order **PI₀-S6** < **PI₁-S6** < **PI₂-S6** < **PI₃-S6**. This result further proved the successful synthesis of azo-PAA.

ATR FTIR spectra were also recorded to confirm the successful synthesis of azo-PIs. The ATR FTIR spectra of **PI_x-S6**

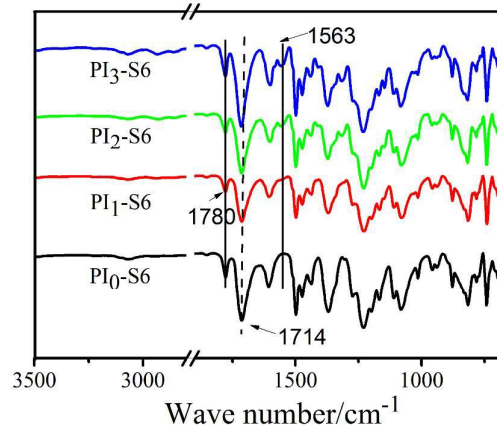


Figure 4. ATR FTIR spectra of **PI_x-S6** films.

films are shown in Figure 4 as representative cases. They were measured after thermal imidization at 250 °C. The ATR FTIR spectra of the other films after imidization are shown in Figures S5–S7. The characteristic IR bands of PAA (carbonyl absorption at ν=1651 cm⁻¹ and a broad carboxylic acid absorption at ν=3387 cm⁻¹) had clearly disappeared in all of the ATR FTIR spectra, indicating the successful conversion of PAAs to PIs. Strong bands at ν=1780 and 1714 cm⁻¹, attributable to the –C=O asymmetrical and symmetrical stretching vibrations of imide rings, were also observed for all

of the azo-PIs. The absorption peak at $\nu=720\text{ cm}^{-1}$ corresponded to imide ring deformation, and the bands at $\nu=1375$ and $1244\text{--}1103\text{ cm}^{-1}$ could be assigned to vibrations of the C(Ph)-N and C-O-C units, respectively. The absorption peak at $\nu=1563\text{ cm}^{-1}$ could be attributed to a stretching vibration of the pyrimidine ring. The increased intensity of this peak at $\nu=1563\text{ cm}^{-1}$ reflected the changes in the molar ratio of Sn/ODA in the respective azo-PI backbones.

3.2. Properties of azo-PIs

3.2.1. Film quality and mechanical properties of azo-PIs

The obtained films were yellow in color, which could be attributed to the azo unit, as shown in Figure 5 for **PIx-S6**, while the others are shown in Figures S8–S10. The average thickness of each azo-PI film was estimated as about 20 μm by means of a film thickness measuring instrument. The mechanical properties of the azo-PI films, including tensile strength, tensile modulus, as well as elongation at break, are summarized in Table S2, except those for **PI₃-S2**, which proved to be too fragile to be subjected to tensile tests. Each result was obtained from five drawing experiments. The tensile strengths were in the range 64–127 MPa, elongations at break were in the range 3.1–9.6%, and tensile moduli were in the range 1.94–3.02 GPa. With increasing amounts of rigid pyrimidyl diamine, the molecular weights of the PIs decreased and their mechanical properties deteriorated.³⁵ However, the collected tensile data demonstrated that the films prepared from these azo-PIs were tough and could be used for further processing as optical coating layers.



Figure 5. Optical photographs of **PIx-S6** films.

3.2.2. Thermal properties of the azo-PIs

The thermal properties of the azo-PIs were evaluated by DSC as well as TGA under a nitrogen atmosphere, and the thermal

data are summarized in Table S1. Figure 6 shows DSC curves for the second heating scans of the azo-PIs. The length of the side chain proved to have little effect on the T_g of azo-PIs. The

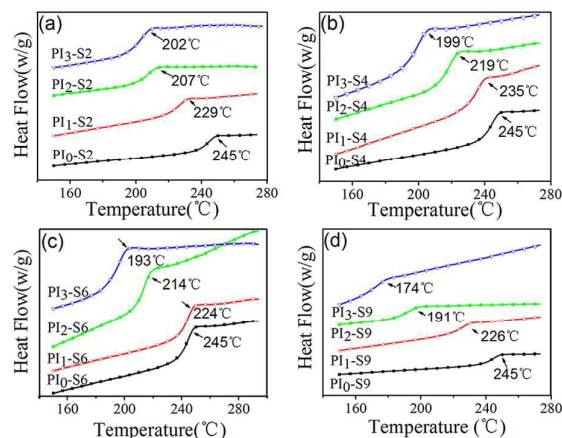


Figure 6. DSC second heating scan curves of the azo-PIs at 20 °C/min.

T_g values decreased with increasing amount of pyrimidyl diamine, which can be attributed to the introduction of more azo side chains. Although the introduction of heterocyclic aromatic structure into PI led to an enhancement of thermal stability, the appending of long side chains resulted in loose chain packing and weak intermolecular interactions. Therefore, the free volume in the polymer system increased, which reduced the T_g values of the azo-PIs.³⁶ Notably, these azo-PIs exhibited better thermal stability, with higher T_g , than that of previously reported azo-PI materials.¹⁷

The thermal stabilities of the azo-PIs were further estimated from the decomposition temperatures corresponding to 5% and 10% weight losses (T_{d5} and T_{d10}), as shown in Figure 7 and summarized in Table S1. **PI₀**, containing no alkyl chain, was thermally stable up to 510 °C. All of the obtained azo-PIs showed high T_{d5} above 370 °C and T_{d10} above 400 °C. The thermal properties of the azo-PIs deteriorated with the introduction of alkoxy side chains. Moreover, their char yields after pyrolysis at 700 °C were higher than 40%. Compared with **PI₀**, the azo-PIs showed two-step weight-loss processes.³⁷ The weight loss associated with the first step was equivalent to the weight of the side chain, indicating that the side chains began to degrade at ca. 400 °C. The second step of weight loss occurred over the same temperature range as the degradation of **PI₀**. This suggests that the first step of weight loss was related to degradation of the side chains, and the second step corresponded to degradation of the PI main chain.

3.2.3. Photo-induced birefringence

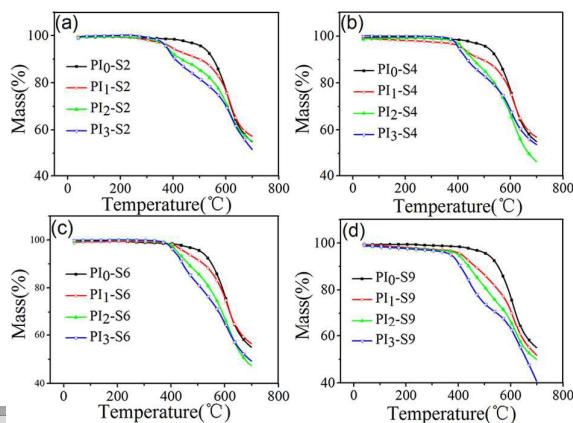


Figure 7. TGA curves of azo-PIs at 20 °C/min in nitrogen.

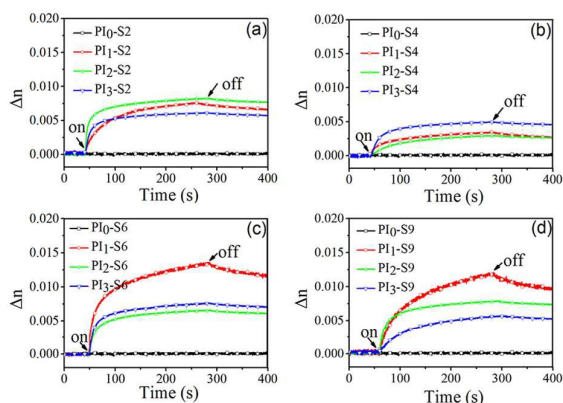


Figure 8. Photo-induced birefringence recorded for thin films of PIs with a 405 nm linearly polarized beam at room temperature. The points at which the pumping light was switched on and off are marked with arrows.

The photo-induced birefringence of the azo-PIs was investigated using a 405 nm laser as pump source. As shown in Figure 8, when the pump beam was switched on, a slow increase in the transmitted light was recorded. The birefringence (Δn) increased with increasing irradiation time and reached a high saturation value after 280 s. The birefringence values of **PI₁-S6** and **PI₁-S9** were found to be higher than those of the other films, with high Δn values of 0.0134 for **PI₁-S6** and 0.0122 for **PI₁-S9** at room temperature. These results clearly proved that the spacer length of the azo units had a significant effect on the photo-induced birefringence, whereby the *trans*-to-*cis* isomerization of the azo groups occurred much less readily in the rigid main chain of PIs with shorter spacer lengths. When the spacer was longer than six methylene units, the effect on birefringence was not obvious, similar to the phenomenon reported by Wu Yiliang.³⁰ The authors studied the effect of spacer length of the azobenzene unit on alignment behavior of liquid crystal polymer was investigated by poly(methyl methacrylate). The results proved that alignment change is more difficult to be generated in the liquid crystal polymer having a short spacer length of azo units. Finally, it was noted that the photo-induced birefringence of the azo-PIs showed a slight decrease after turning off the pump light at room temperature. The highest photo-induced birefringence value among the **PI_x-S6** was that of the **PI₁-S6** film, which had a relatively low azo content of 10%. It is assumed that most of the molecules were located in larger free volumes when undergoing isomerization. The decrease in birefringence with increasing azo content can be attributed to the lower free volume, which limited in-plane isomerization of the azo group, thereby reducing the efficiency of the photo-induced birefringence process.³⁸

In order to reveal the influence of temperature on the birefringence of the azo-PIs, **PI₁-S6** and **PI₁-S9** were chosen as samples. As shown in Figure 9, when the pump beam was switched on, a faster increase in the transmitted light was recorded at 100 °C than at 25 °C. The birefringence at 100 °C was higher than that at 25 °C for both azo-PIs. This could be attributed to certain motions of the azo groups, such as thermally induced *cis*-to-*trans* isomerization.³⁹ In addition, switching off the pump beam led to a faster decay for azo-PIs

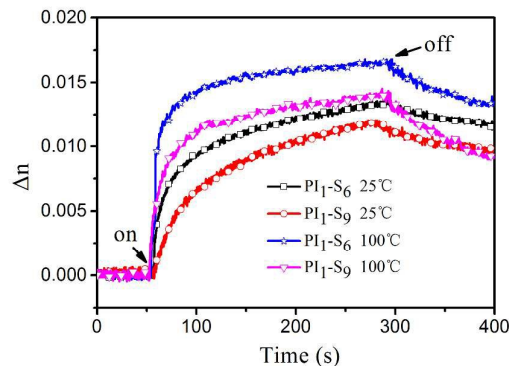


Figure 9. Photo-induced birefringence of **PI₁-S6** and **PI₁-S9** recorded with a 405 nm linearly polarized beam at 25 and 100 °C.

at 100 °C. The decay for **PI₁-S9** was more obvious. This is because the longer spacer is beneficial for molecular movement of the azo group.

The samples irradiated at different temperatures were annealed to further investigate the thermal stability of the photo-induced birefringence. As shown in Figure 10, for **PI₁-S6**, the birefringence decays were monitored at 25 °C, 100 °C, and 150 °C. A characteristic feature of these decays was that none of them reached the zero level after relaxation in darkness. According to previous reports, this was because, after the reorientation, some of the molecules remained “frozen” in their positions, which depended on the T_g value of the polymer.⁴⁰ Szukalski et al. studied the photo-induced birefringence of pyrazoline-doped PMMA, revealing that the birefringence decreased to 54.7% after relaxation in darkness for 200 s at room temperature.⁴¹ Rochon studied the optically induced birefringence of azo-aromatic polymers. The transmitted signal was observed to decrease to 60% of the saturation value just 10 s after the writing beam was turned off.⁴⁰ In this work, after relaxation treatment for 1000 s, the birefringence was observed to decrease to 59.4% of the saturation value at 25 °C. This result indicated that some of the molecules did not remain oriented on a long-term basis; nevertheless, a significant number remained and the birefringence was observed to be quite stable for a long

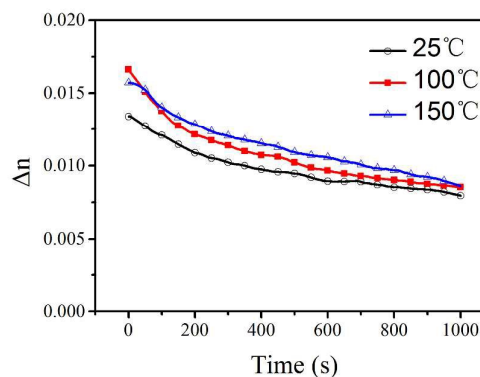


Figure 10. Changes in optical birefringence during dark relaxation processes for **PI₁-S6** after exposure to different temperatures.

time³⁷. The birefringence decay to 54.8% of the saturation value at 150 °C was comparable to that at room temperature. These results proved that the photo-induced birefringent films have excellent thermal stability.

Conclusions

In conclusion, this work demonstrates a series of new optically anisotropic azo-PIs prepared by directly appending different lengths of azo chains to pyrimidyl diamine, which show good combined properties of both polyimide and azo. All of the azo-PI films showed outstanding thermal stability, with high T_{d5} values of about 400 °C in nitrogen and T_g around 200 °C. Azo-PI films fabricated through a casting method showed good dimensional stability, moderate to high thermal stability, and good mechanical performance. The *trans*-to-*cis* isomerization of the azo group (N=N) occurred less readily in the rigid main chains of azo-PIs that contained azo units with short spacer lengths. When the spacer length was longer than six methylene units, its effect on the birefringence was not obvious. Obvious photo-induced birefringence (0.0166) was measured for **PI₁-S6** at 100 °C by using a continuous 405 nm laser as the pump light. Our as-prepared azo-PI films displayed high photo-induced birefringence as well as good thermostability. The resultant azo-PI films are expected to have promising potential applications in optical materials.

Conflict of interest

The authors declare no competing financial interests.

Acknowledgements

The authors are grateful for financial support from the National Science Foundation of China (51733007 and 21574081) and 973 Projects (2014CB643605).

References

- 1 K. G. Yager and C. J. Barrett, Novel photo-switching using azobenzene functional materials, *J. Photochem. Photobiol., A*, 2006, **182**, 250-261.
- 2 M. O'Neill and S. M. Kelly, Liquid crystals for charge transport luminescence, and photonics, *Adv Mater*, 2003, **15**, 1135-1146.
- 3 A. Natansohn and P. Rochon, Photoinduced motions in azo-containing polymers, *Chem. Rev.*, 2002, **102**, 4139-4175.
- 4 M. Shi, J. Mack, L. Yin, X. Y. Wang and Z. Shen, Photoisomerization and optical behavior study of a subphthalocyanine-bisazobenzene-subphthalocyanine triad with visible-light response, *J. Mater. Chem. C*, 2016, **4**, 7783-7789.
- 5 J. Vapaavuori, R. H. Ras, M. Kaivola, C. G. Bazuin and A. Priimagi, From partial to complete optical erasure of azobenzene-polymer gratings: effect of molecular weight, *J. Mater. Chem. C*, 2015, **3**, 11011-11016.
- 6 B. Sapich, A. B. E. Vix, J. P. Rabe and J. Stumpe, Photoinduced self-organization and photoorientation of a LC main-chain polyester containing azobenzene moieties, *Macromolecules*, 2005, **38**, 10480-10486.
- 7 A. Bobrovsky, V. Shibaev, V. Hamplova, M. Kaspar and M. Glogarova, Chiroptical and photooptical properties of a novel side-chain azobenzene-containing LC polymer, *Monatsh. Chem.*, 2009, **140**, 789-799.
- 8 N. J. Li, J. M. Lu, X. W. Xia, Q. F. Xu and L. H. Wang, Synthesis and the third-order nonlinear optical properties of soluble polymers with different substituted azobenzene side chains, *Polymer*, 2009, **50**, 428-433.
- 9 S. Furumi and K. Ichimura, Photogeneration of high pretilt angles of nematic liquid crystals by non-polarized light irradiation of azobenzene-containing polymer films, *Adv Funct Mater*, 2004, **14**, 247-254.
- 10 A. Bobrovsky, K. Mochalov, A. Chistyakov, V. Oleinikov and V. Shibaev, AFM study of laser-induced crater formation in films of azobenzene-containing photochromic nematic polymer and cholesteric mixture, *J. Photochem. Photobiol., A*, 2014, **275**, 30-36.
- 11 S. Z. Yang, K. Yang, A. Jain, R. Nagarajan and J. Kumar, Patterning flexible substrates using surface relief structures in azobenzene functionalized polymer films, *J. Macromol. Sci.*, 2008, **45**, 938-941.
- 12 K. Sakamoto, K. Usami and K. Miki, Photoalignment efficiency enhancement of polyimide alignment layers by alkyl-amine vapor treatment, *Appl. Phys. Express*, 2014, **7**, 081701.
- 13 N. Hosono, M. Yoshikawa, H. Furukawa, K. Totani, K. Yamada, T. Watanabe and K. Horie, Photoinduced deformation of rigid azobenzene-containing polymer networks, *Macromolecules*, 2013, **46**, 1017-1026.
- 14 I. Sava, A. Burescu, I. Stoica, V. Musteata, M. Cristea, I. Mihaila and V. Pohoatab, Properties of some azo-copolyimide thin films used in the formation of photoinduced surface relief gratings, *RSC Adv.*, 2015, **5**, 10125-10133.
- 15 K. Zlatanova, P. Markovsky, I. Spassova and G. Danev, Photoinduced changes in methyl orange polyimide layers, *Opt. Mater.*, 1996, **5**, 279-283.
- 16 E. Schab-Balcerzak, M. Siwy, M. Kawalec, A. Sobolewska, A. Chamera and A. Miniewicz, Synthesis, characterization, and study of photoinduced optical anisotropy in polyimides containing side azobenzene units, *J. Phys. Chem. A*, 2009, **113**, 8765-8780.
- 17 E. Schab-Balcerzak, M. Grucela-Zajac, A. Kozanecka-Szmigiel and K. Switkowski, Poly(etherimide)s and poly(esterimide)s containing azobenzene units: Characterization and study of photoinduced optical anisotropy, *Opt. Mater.*, 2012, **34**, 733-740.
- 18 A. Kozanecka-Szmigiel, J. Konieczkowska, D. Szmigiel, K. Switkowski, M. Siwy, P. Kuszewski and E. Schab-Balcerzak, Photoinduced birefringence of novel azobenzene poly(esterimide)s; the effect of chromophore substituent and excitation conditions, *Dyes Pigm.* 2015, **114**, 151-157.
- 19 J. Konieczkowska, E. Schab-Balcerzak, M. Siwy, K. Switkowski and A. Kozanecka-Szmigiel, Large and highly stable photoinduced birefringence in poly(amideimide)s with two azochromophores per structural unit, *Opt. Mater.* 2015, **39**, 199-206.
- 20 J. Konieczkowska, H. Janeczek, A. Kozanecka-Szmigiel and E. Schab-Balcerzak, Poly(amic acid)s and their poly(amide imide) counterparts containing azobenzene moieties: Characterization, imidization kinetics and photochromic properties, *Mater. Chem. Phys.* 2016, **180**, 203-212.
- 21 S. J. Zhang, Y. F. Li, D. X. Yin, X. L. Wang, X. Zhao, Y. Shao and S. Y. Yang, Study on synthesis and characterization of novel polyimides derived from 2,6-Bis(3-aminobenzoyl) pyridine, *Eur. Polym. J.*, 2005, **41**, 1097-1107.

- 22 J. W. Xia, J. H. Li, G. P. Zhang, X. L. Zeng, F. F. Niu, H. P. Yang, R. Sun and C. P. Wong, Highly mechanical strength and thermally conductive bismaleimide–triazine composites reinforced by Al_2O_3 @polyimide hybrid fiber, *Composites Part A*, 2016, **80**, 21-27.
- 23 A. Javadi, Z. Najjar, S. Bahadori, V. Vatanpour, A. Malek, E. Abouzari-Lotfde and A. Shokravi, High refractive index and low-birefringence polyamides containing thiazole and naphthalene units, *RSC Adv.*, 2015, **5**, 91670-91682.
- 24 T. Matsumoto, K. Nishimura and T. Kurosaki, Ladder-type polyimides based on diaminodibenzofurane, *Eur. Polym. J.*, 1999, **35**, 1529-1535.
- 25 A. X. Xia, G. H. Lü, X. P. Qiu, H. Q. Guo, J. Y. Zhao, M. X. Ding and L. X. Gao, Syntheses and properties of novel polyimides derived from 2-(4-aminophenyl)-5-aminopyrimidine, *J. Appl. Polym. Sci.*, 2006, **102**, 5871-5876.
- 26 L. L. Chen, S. H. Jiang, J. Chen, F. Chen, Y. Y. He, Y. M. Zhu and H. Q. Hou, Single electrospun nanofiber and aligned nanofiber belts from copolyimide containing pyrimidine units, *New J. Chem.*, 2015, **39**, 8956-8965.
- 27 K. Nakabayashi, T. Imai, M. C. Fu, S. Ando, T. Higashihara and M. Ueda, Synthesis and characterization of poly(phenylene thioether)s containing pyrimidine units exhibiting high transparency, high refractive indices, and low birefringence, *J. Mater. Chem. C*, 2015, **3**, 7081-7087.
- 28 N. You, T. Higashihara, Y. Oishi, S. Ando and M. Ueda, Highly refractive poly(phenylene thioether) containing triazine unit, *Macromolecules*, 2010, **43**, 4613-4615.
- 29 C. B. Wang, Y. Guan, D. B. Tian, G. D. Dang, D. M. Wang, C. H. Chen and H. W. Zhou, Highly transparent polyimides derived from 2-phenyl-4,6-bis(4-aminophenoxy)pyrimidine and 1,3-bis(5-amino-2-pyridinoxy)benzene: preparation, characterization, and optical properties, *RSC Adv.*, 2015, **5**, 103246-103254.
- 30 Y. L. Wu, Y. Demachi, O. Tsutsumi, A. Kanazawa, T. Shiono and T. Ikeda, Photoinduced alignment of polymer liquid crystals containing azobenzene moieties in the side chain. 2. Effect of spacer length of the azobenzene unit on alignment behavior, *Macromolecules*, 1998, **31**, 1104-1108.
- 31 J. Stumpe, T. Fischer and H. Menzel, Langmuir-Blodgett films of photochromic polyglutamates. 9. Relation between photochemical modification and thermotropic properties, *Macromolecules*, 1996, **29**, 2831-2842.
- 32 S. F. Xiao, X. M. Lu, Q. H. Lu and B. Su, Photosensitive liquid-crystalline supramolecules self-assembled from ionic liquid crystal and polyelectrolyte for laser-induced optical anisotropy, *Macromolecules*, 2008, **41**, 3884-3892.
- 33 J. Wu, X. M. Lu, Z. Y. Yi, F. Shan and Q. H. Lu, Anisotropic fluorescence emission of ionic complex induced by the orientation of azobenzene unit, *Macromolecules*, 2013, **46**, 3376-3383.
- 34 I. Gillerman and B. Fischer, Investigations into the origin of the molecular recognition of several adenosine deaminase inhibitors, *J. Med. Chem.*, 2011, **54**, 107-121.
- 35 A. I. Barzic, R. D. Rusu, I. Stoica and M. D. Damaceanu, Chain flexibility versus molecular entanglement response to rubbing deformation in designing poly(oxadiazolenaphthylimide)s as liquid crystal orientation layers, *J. Mater. Sci.*, 2014, **49**, 3080-3098.
- 36 S. L. Xia, L. F. Yi, Z. Sun and Y. H. Wang, The effect of phthalimide side chains on the thermal stability and rubbing resistance of polyimide used as a liquid crystal vertical alignment layer, *J. Polym. Res.*, 2013, **20**, 219.
- 37 S. I. Kim, M. Ree, T. J. Shin and J. C. Jung, Synthesis of New Aromatic Polyimides with various side chains containing a biphenyl mesogen unit and their abilities to control liquid-crystal alignments on the rubbed surface, *J. Polym. Sci., Part A: Polym. Chem.*, 1999, **37**, 2909-2921.
- 38 J. Wu, X. M. Lu, F. Shan, J. F. Guan and Q. H. Lu, Photoresponding ionic complex containing azobenzene chromophore for use in birefringent film, *Chin. Chem. Lett.*, 2014, **25**, 15-18.
- 39 V. Börger, O. Kuliskovska, K. G. Hubmann, J. Stumpe, M. Huber and H. Menzel, Novel polymers to study the influence of the azobenzene content on the photo-induced surface relief grating formation, *Macromol. Chem. Phys.*, 2005, **206**, 1488-1496.
- 40 P. Rochon, J. Gosselin, A. Natansohn and S. Xie, Optically induced and erased birefringence and dichroism in azoaromatic polymers, *Appl. Phys. Lett.*, 1992, **60**, 4-5.
- 41 A. Szukalski, K. Haupa, A. Miniewicz and J. Mysliwiec, Photoinduced birefringence in PMMA polymer doped with photoisomerizable pyrazoline derivative, *J. Phys. Chem. C*, 2015, **119**, 10007-10014.